

## Research Article

Zhongyu Zhang\*, Meng Chen, Mingqiong Tong, Wan Sun, Pingxuan Dong, Xinfeng Song and Xiaoyue Wang

# Syntheses, crystal structure, thermal behavior, and anti-tumor activity of three ternary metal complexes with 2-chloro-5-nitrobenzoic acid and heterocyclic compounds

<https://doi.org/10.1515/hc-2022-0011>

received November 01, 2021; accepted March 16, 2022

**Abstract:** Three complexes, namely complex (1), complex (2), and complex (3), were synthesized and characterized by X-ray diffraction, thermogravimetric study, and elemental study. Complex (1) comprises discrete binuclear clusters, where two oxygen atoms of 2-chloro-5-nitrobenzoic acid bridge the two copper atoms. Complex (2) is a six-coordination structure consisting of four nitrogen atoms and two oxygen atoms in 2-chloro-5-nitrobenzoic acid and 1,10-phenanthroline to furnish a twisted octahedron. Complex (3) is a six-coordination structure consisting of four oxygen atoms and two nitrogen atoms from the 2-chloro-5-nitrobenzoic acid, methanol, and 2,2'-dipyridyl to furnish a distorted octahedral geometry. Metal complexes' anti-tumor activity was also investigated by the MTT assay. Of the complexes tested, complex (1) could induce apoptosis in these A549 lung cancer and Caco-2 colon adenocarcinoma cells and complex (2) could induce apoptosis in Caco-2 colon adenocarcinoma cells. CCDC for complex (1) was 1543354, CCDC for complex (2) was 1546991, and CCDC for complex (3) was 1543417.

**Keywords:** metal complexes, 2-chloro-5-nitrobenzoic acid, 1,10-phenanthroline, 2,2'-dipyridyl, anti-tumor activity

## 1 Introduction

The treatment of cancer has long been a global problem. For years, metallic drugs have been applied clinically. For instance, cisplatin, a platinum compound, is employed in chemotherapy for various cancers [1–3]. However, severe side effects, such as ototoxicity, nephrotoxicity, or electrolyte disorders, occur when cisplatin-based chemotherapy is used [4,5]. Therefore, many researchers are trying to design novel anticancer drugs based on potential metals to improve clinical effectiveness, tackle resistance, and reduce toxicity [6]. Heterocyclic compounds play an important role in many biochemical processes and are widespread in nature [7]. These compounds are notable for several reasons, the most important of which is their biological activities. Besides, numerous drugs are heterocyclic compounds [8]. 1,10-Phenanthroline, 2,2'-dipyridyl, and their substituted derivatives interfere with the functions of many biological systems [9,10]. When the N-chelate base without metal is found with the biological activity, it is generally considered to be associated with the separation of trace metals, and the resulting metal complexes are active species. Interests in benzoic acid arise from its biological importance and chemical properties. Benzoic acids show considerable important biological activity (e.g., antibacterial, antifungal, antiviral, herbicide, anti-inflammatory, anti-tumor, and anticancer activities) [11,12]. 2-Chloro-5-nitrobenzoic acid can be combined with various metals (e.g., lead, copper, manganese, and nickel), and it exhibits excellent physical properties [13–15].

This study speculates that synthetic forms of Cu(II), Ni(II), and Mn(II) with 2-chloro-5-nitro-benzoic acid and

\* **Corresponding author: Zhongyu Zhang**, Shandong Provincial Engineering Laboratory of Novel Pharmaceutical Excipients, Sustained and Controlled Release Preparations, Department of Medicine and Nursing, Dezhou University, Decheng District, Dezhou 253023, China, e-mail: dzzhangzhongyu@163.com

**Meng Chen:** Department of Pediatric Surgery, Qilu Hospital of Shandong, University Dezhou Hospital, Decheng District, Dezhou 253014, China

**Mingqiong Tong, Wan Sun, Pingxuan Dong, Xinfeng Song, Xiaoyue Wang:** Shandong Provincial Engineering Laboratory of Novel Pharmaceutical Excipients, Sustained and Controlled Release Preparations, Department of Medicine and Nursing, Dezhou University, Decheng District, Dezhou 253023, China

heterocyclic compounds may induce the apoptosis of cancer cells. To verify this hypothesis, three ternary metal complexes were fabricated in anhydrous solvent and their crystal structures were determined. These complexes were characterized and assessed, and their abilities to induce the apoptosis of A549 human lung cancer and Caco-2 human colon adenocarcinoma cells were compared. Among the complexes tested, complex (1) could induce apoptosis in the A549 lung cancer and Caco-2 colon adenocarcinoma cells; complex (2) could induce apoptosis in Caco-2 colon adenocarcinoma cells.

## 2 Results and discussion

### 2.1 Method of preparation

The binary metal complexes of 2-chloro-5-nitrobenzoic acid were synthesized by the direct synthesis method, and the second ligand was added to the solution of the aforementioned binary metal complex. The ternary metal complex was synthesized by the component exchange method. Single crystals of the ternary metal complex were obtained by the natural volatilization culture.

### 2.2 Description of crystal structure

The selected bond lengths and bond angles of complexes are listed in Tables 1 and 2 [16]. The normal chem draw structure of synthesized metal complexes is shown in Figure 1. Crystal structures of the three complexes are presented in Figures 2–4. Besides, packing diagrams of the three complexes are shown in Figures 5–7.

Figure 2 shows that complex (1) is a binuclear Cu(II) complex. The copper atom is coordinated with three oxygen atoms and two nitrogen atoms from the 2-chloro-5-nitrobenzoic acid and 1,10-phenanthroline to form a twisted square cone configuration. The two Cu(II) centers are bridged together by the two oxygen atoms from 2,2-chloro-5-nitrobenzoic acid molecules. The oxygen atom of the deprotonated COOH groups is bridged the two Cu(II) centers directly. This bridge keeps together the two Cu(II) centers forming complex (1). In the complex (1), the bond angles of O3a–Cu1a–N1a, O3a–Cu1a–N2a, O1a–Cu1a–O3a, O1a–Cu1a–N1a, O1a–Cu1a–N1a, O1a–Cu1a–O3b and N1a–Cu1a–O3b are 93.179(16)°, 174.92(14)°, 90.20(15)°, 175.31(15)°, 95.494(137)° and 88.402(148)°, respectively, the Cu(II) is five coordinated by threeoxygen and two nitrogen atoms from the three 2-chloro-5-nitrobenzoic acid ligands, and 1,10-phenanthroline to furnish a distorted square-pyramidal geometry. Figure 5 shows that

**Table 1:** Selected bond lengths (Å) of the complexes obtained from experiment

Complex (1)		Complex (2)		Complex (3)	
Bond	Length/Å	Bond	Length/Å	Bond length	Length/Å
Cu1a–O3a	1.977 (3)	Mn–O1	2.096 (2)	Ni–O3a	2.130 (6)
Cu1a–O1a	1.930 (3)	Mn1–O3	2.099 (3)	Ni–O3b	2.130 (6)
Cu1a–N1a	2.018 (4)	Mn1–N4	2.245 (3)	Ni–O1a	2.031 (7)
Cu1a–N2a	2.009 (4)	Mn1–N2	2.277 (3)	Ni–O1b	2.031 (7)
Cu1a–O3b	1.977 (3)	Mn1–N3	2.293 (3)	Ni–N2a	2.060 (8)
Cu1b–O3a	1.977 (3)	Mn1–N1	2.326 (3)	Ni–N2b	2.060 (8)
Cu1b–O1b	1.930 (3)	N1–C24	1.314 (5)	O3a–C13a	1.428 (13)
Cu1b–N1b	2.018 (4)	N1–C25	1.357 (5)	O3b–C13b	1.428 (13)
Cu1b–N2b	2.009 (4)	N2–C15	1.325 (5)	O1a–C1a	1.235 (11)
Cu1b–O3b	1.977 (3)	N2–C16	1.357 (5)	O1b–C1b	1.235 (11)
C1b–O1b	1.283 (6)	N3–C27	1.324 (5)	O2a–C1a	1.258 (12)
C1a–O1a	1.283 (6)	N3–C37	1.355 (4)	O2b–C1b	1.258 (12)
C8a–O3a	1.299 (6)	N4–C36	1.325 (5)	N2a–C8a	1.325 (14)
C8b–O3b	1.299 (6)	N4–C38	1.355 (4)	N2a–C12a	1.337 (12)
C8b–O4b	1.210 (6)	O3–C8	1.261 (4)	N2b–C8b	1.325 (14)
C8a–O4a	1.210 (6)	O1–C1	1.269 (4)	N2a–C12b	1.337 (12)
C1a–O2a	1.223 (6)	O4–C8	1.213 (4)	C1a–C2a	1.510 (13)
C1b–O2b	1.223 (6)	O2–C1	1.230 (4)	C1b–C2b	1.510 (13)

**Table 2:** Selected bond angles ( $^{\circ}$ ) of the complexes obtained from experiment

Complex (1)		Complex (2)		Complex (3)	
Bond angle	Angles ( $^{\circ}$ )	Bond angle	Angles ( $^{\circ}$ )	Bond angle	Angles ( $^{\circ}$ )
O3a–Cu1a–N1a	93.17 (16)	O1–Mn1–O3	90.16 (10)	O1a–Ni–O1b	93.7 (4)
O3a–Cu1a–N2a	174.92 (14)	O1–Mn1–N4	91.11 (11)	O1b–Ni–O3b	88.2 (3)
O1a–Cu1a–O3a	90.20 (15)	O3–Mn1–N4	108.54 (11)	O1b–Ni–O3a	87.4 (3)
O1a–Cu1a–N1a	175.31 (15)	O1–Mn1–N2	102.06 (10)	O1a–Ni–O3b	87.4 (3)
O1a–Cu1a–N2a	94.66 (16)	O3–Mn1–N2	86.56 (11)	O1a–Ni–O3a	88.2 (3)
N2a–Cu1a–N1a	81.89 (17)	N4–Mn1–N2	160.08 (11)	O1a–Ni–N2a	172.0 (3)
O1a–Cu1a–O3b	95.494 (137)	O1–Mn1–N3	163.76 (11)	O1b–Ni–N2a	93.5 (3)
O3a–Cu1a–O3b	78.345 (131)	O3–Mn1–N3	93.90 (10)	O1a–Ni–N2b	93.5 (3)
N1a–Cu1a–O3b	88.402 (148)	N4–Mn1–N3	72.69 (10)	O1a–Ni–N2b	172.0 (3)
N2a–Cu1a–O3b	102.599 (145)	N2–Mn1–N3	93.89 (10)	O3a–Ni–O3b	173.6 (4)
C8a–O3a–Cu1a	115.3 (3)	O1–Mn1–N1	92.25 (10)	N2a–Ni–O3a	95.4 (3)
C1a–O1a–Cu1a	123.1 (3)	O3–Mn1–N1	158.34 (12)	N2a–Ni–O3b	89.6 (3)
C25a–N1a–Cu1a	112.7 (3)	N4–Mn1–N1	92.94 (12)	N2b–Ni–O3b	95.4 (3)
C24a–N1a–Cu1a	129.5 (3)	N2–Mn1–N1	71.89 (12)	N2b–Ni–O3a	89.6 (3)
C24a–N1a–C25a	117.8 (4)	N3–Mn1–N1	89.75 (9)	N2a–Ni–N2b	79.4 (5)
C26a–N2a–Cu1a	112.5 (3)	C8–O3–Mn1	134.4 (2)	C1b–O1b–Ni	124.2 (7)
C15a–N2a–Cu1a	129.8 (3)	C1–O1–Mn1	129.6 (2)	C13b–O3b–Ni	120.4 (7)
O3b–Cu1b–N1b	93.17 (16)	C24–N1–C25	117.9 (3)	C12b–N2b–Ni	114.9 (7)
O3b–Cu1b–N2b	174.92 (14)	C24–N1–Mn1	126.8 (3)	C8b–N2b–Ni	124.8 (7)
O1b–Cu1b–O3b	90.20 (15)	C25–N1–Mn1	115.3 (3)	C1a–O1a–Ni	124.2 (7)
O1b–Cu1b–N1b	175.31 (15)	C36–N4–C38	118.5 (3)	C13a–O3a–Ni	120.4 (7)
O1b–Cu1b–N2b	94.66 (16)	C36–N4–Mn1	125.0 (2)	C12a–N2a–Ni	114.9 (7)
N2b–Cu1b–N1b	81.89 (17)	C38–N4–Mn1	116.5 (2)	C8a–N2a–Ni	124.8 (7)
O1b–Cu1b–O3a	95.494 (137)	C27–N3–C37	118.2 (3)	C8a–N2a–C12a	120.1 (9)
O3b–Cu1b–O3a	78.345 (131)	C27–N3–Mn1	126.8 (3)	O5a–N1a–O4a	123.8 (10)
N1b–Cu1b–O3a	88.402 (148)	C37–N3–Mn1	115.0 (2)	O5a–N1a–C6a	116.9 (10)
N2b–Cu1b–O3a	102.599 (145)	C15–N2–C26	118.4 (3)	O4a–N1a–C6a	119.3 (9)
C8b–O3b–Cu1b	115.3 (3)	C15–N2–Mn1	124.8 (3)	C8b–N2b–C12b	120.1 (9)
C1b–O1b–Cu1b	123.1 (3)	C26–N2–Mn1	116.8 (2)	O5b–N1b–O4b	123.8 (10)
C25b–N1b–Cu1b	112.7 (3)	N4–C38–C33	122.1 (4)	O5b–N1b–C6b	116.9 (10)
C24b–N1b–Cu1b	129.5 (3)	N4–C38–C37	118.1 (3)	O4b–N1b–C6b	119.3 (9)
C24b–N1b–C25b	117.8 (4)	C33–C38–C37	119.8 (3)	O1a–C1a–O2a	126.6 (9)
C26b–N2b–Cu1b	112.5 (3)	C7–C2–C3	118.4 (4)	O1b–C1b–O2b	126.6 (9)
C15b–N2b–Cu1b	129.8 (3)	C7–C2–C1	118.2 (3)	O2a–C1a–C2a	116.3 (8)

the molecules are connected in stretched chains parallel to axis *a* and axis *c* via short contact and intermolecular  $\pi$ – $\pi$  interactions. The three-dimensional structure of complex (1) is constituted by van der Waals bonds [17,18].

Figure 3 shows that complex (2) is a neutral mono-nuclear complex. Complex (2) is a six-coordination structure consisting of two oxygen atoms and four nitrogen atoms in 2-chloro-5-nitrobenzoic acid and 1,10-phenanthroline to furnish a twisted octahedron. There are two five-element chelating rings (ring 1: Mn–N2–C26–C25–N1 ring 2: Mn–N3–C37–C38–N4). In the complex (2), the bond angles of N4–Mn1–N2, O1–Mn1–N3, and O3–Mn1–N1 are 160.08 (11) $^{\circ}$ , 163.76 (11) $^{\circ}$ , 158.34 (12) $^{\circ}$  respectively. The Mn (II) is six coordinated by two oxygen and four nitrogen atoms from the two 2-chloro-5-nitrobenzoic acid ligands and two 1,10-phenanthroline to furnish a distorted octahedron geometry. Figure 6 shows that the molecules

are connected in stretched chains parallel to axis *a* and axis *b* by intermolecular  $\pi$ – $\pi$  interactions and via van der Waals bonds. The three-dimensional structure of complex (2) is assembled by short contact [19,20].

Figure 4 shows that complex (3) is a neutral mono-nuclear complex as well. In complex (3), Ni(II) locates in a distorted octahedral geometry coordinated with six-bond 2N atoms from 2,2'-dipyridyl, 2O atoms from methanol, and two carboxylate O atoms from 22-chloro-5-nitrobenzoic acid molecules. There is one five-membered chelate ring [ring 1: Ni–N2a–C12a–C12b–N2b]. In the complex (3), the bond angles of O1a–Ni–N2a, O1a–Ni–N2b, and O3a–Ni–O3b are 172.0 (3) $^{\circ}$ , 172.0 (3) $^{\circ}$ , 173.6 (4) $^{\circ}$  respectively. The Ni (II) is six coordinated by four oxygen and two nitrogen atoms from the 2-chloro-5-nitrobenzoic acid ligands, methanol and 1,10-phenanthroline to furnish a distorted octahedron geometry. Figure 7 shows that the molecules are connected

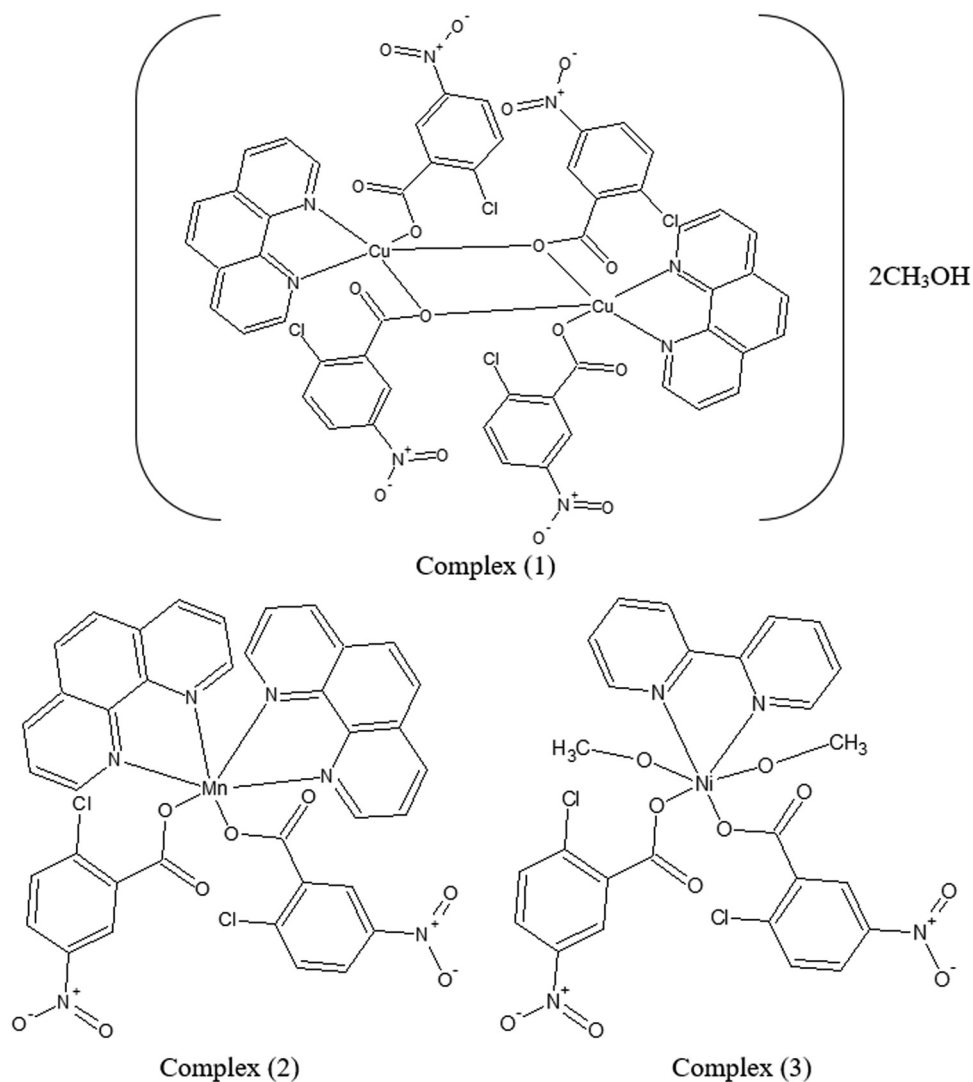


**Figure 1:** Chemical structures of synthesized metal complexes.

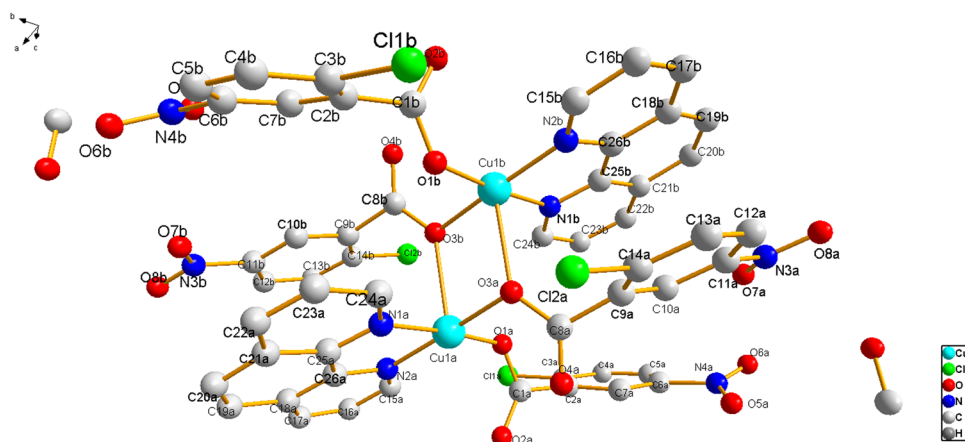


**Figure 2:** The structure of complex (1) and the atom-numbering scheme.

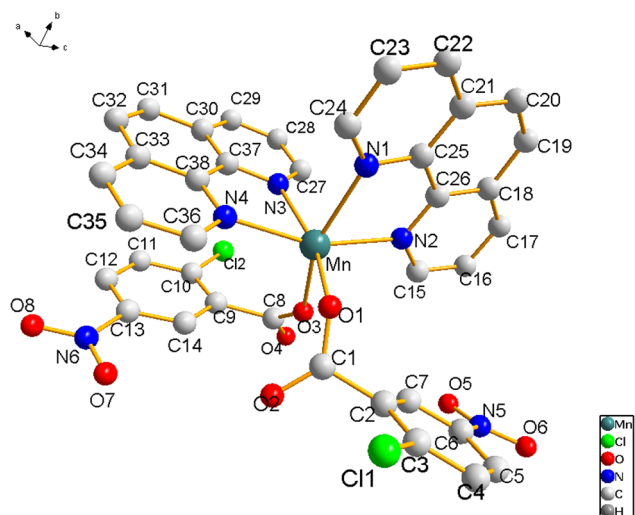


**Figure 3:** The structure of complex (2) and the atom-numbering scheme.

in stretched chains parallel to axis *a* and axis *c* by intermolecular  $\pi$ - $\pi$  interactions and via van der Waals bonds. The three-dimensional structure of complex (3) is assembled by short contact [21].

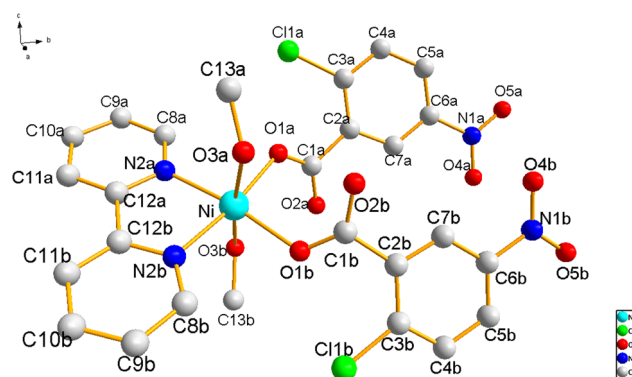


**Figure 4:** The structure of complex (3) and the atom-numbering scheme.

## 2.3 Thermal studies

In the presence of  $N_2$ , the thermal analysis of the complexes was conducted at a temperature from 25 to 1,000°C [22]. As shown in Figure 8, the TGA curve of complex (1) reveals that the mass decreases in two steps with the rise in temperature and the thermal stability of the compound can be up to 226°C. The TGA curve of complex (2)

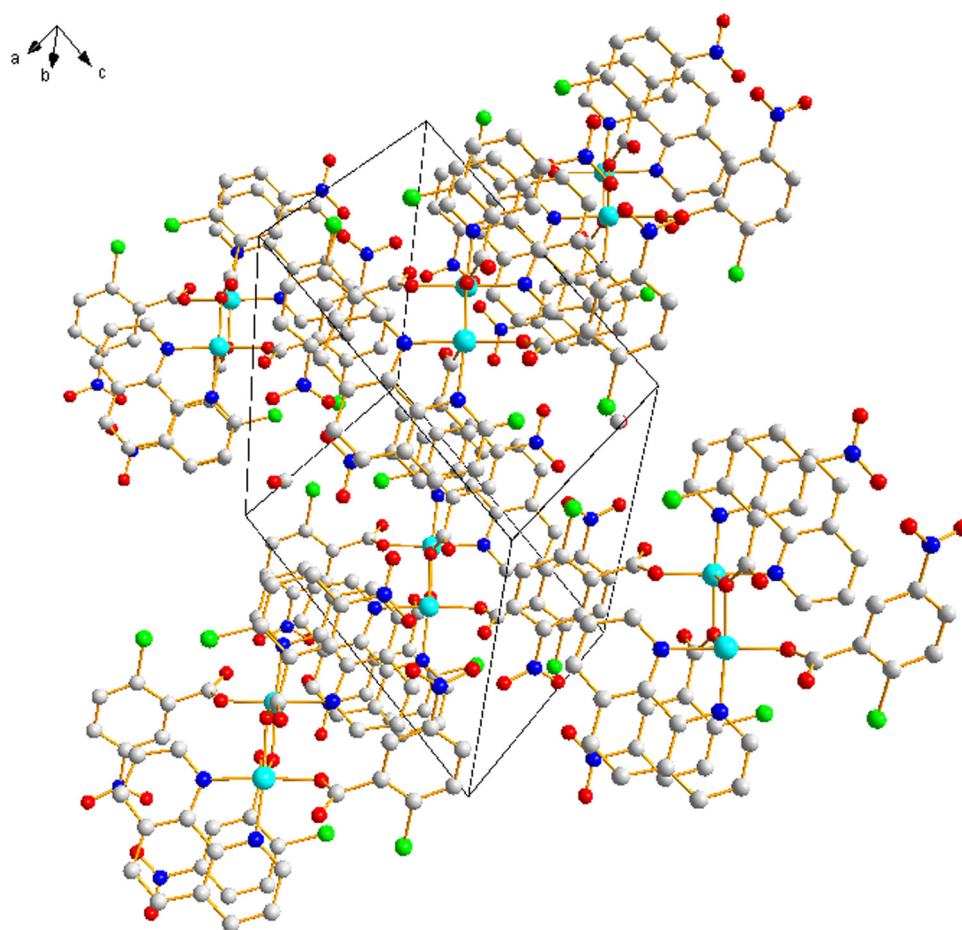


**Figure 5:** Packing diagram of the unit cell of complex (1).

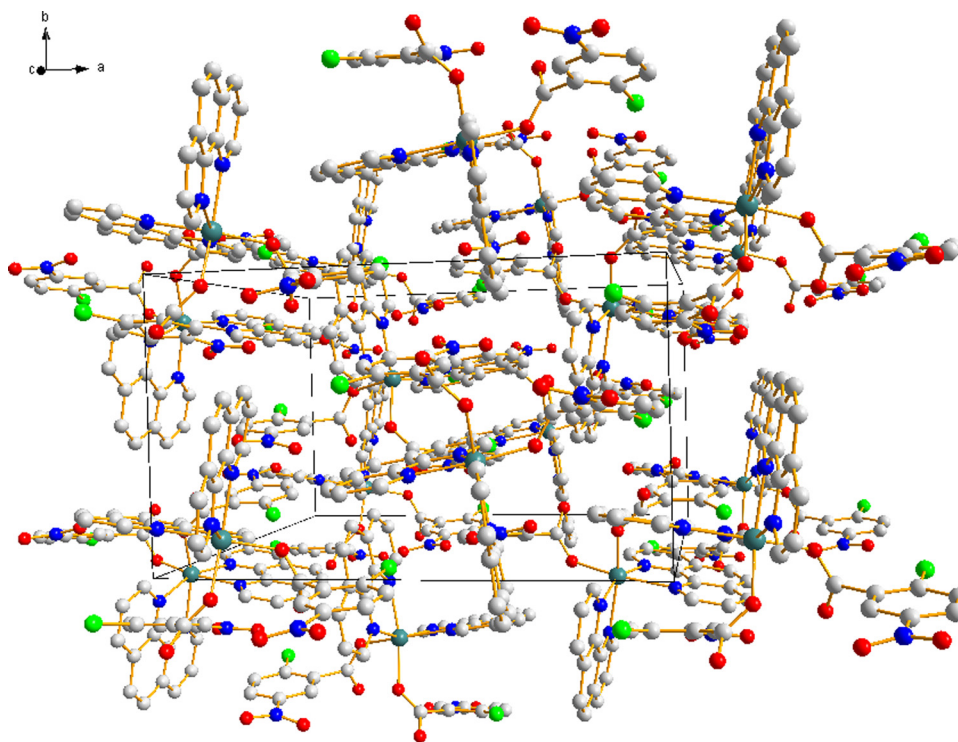


Figure 6: Packing diagram of the unit cell of complex (2).

suggests that the mass decreases in two steps with the rise in temperature and the thermal stability of the compound can reach 270°C. The TGA curve of complex (3) reveals that the mass decreases in two steps with the rise in temperature and the thermal stability of the compound can be up to 120°C [23].

## 2.4 Study on anti-tumor activity

Some important anti-tumor drugs (e.g., cisplatin) have a metal center. These drugs have been employed for years to treat all types of human cancers [24,25]. In a previous study, some Mn(II) and Cu(II) complexes that suppress

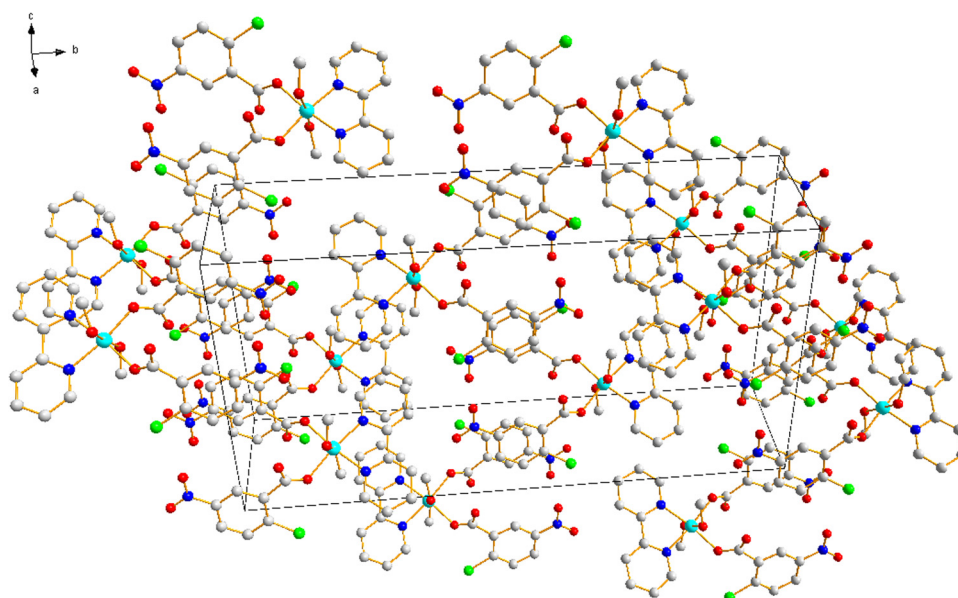


Figure 7: Packing diagram of the unit cell of complex (3).

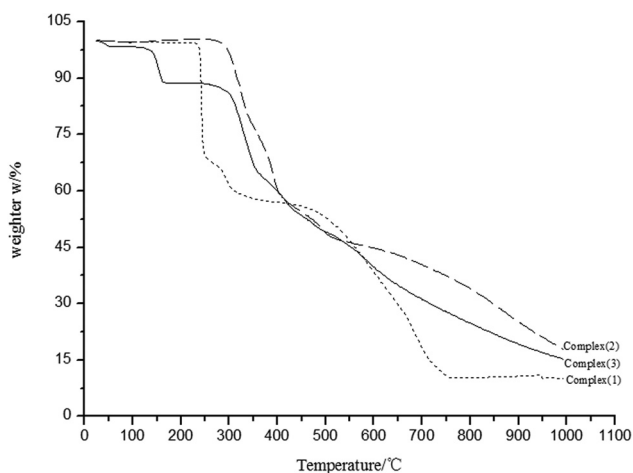


Figure 8: The TGA curve for the complexes.

the proliferation of cancer cells were reported [26,27]. Here, whether the three novel complexes (1), (2), and (3) can suppress the proliferative abilities was studied. A549 and Caco-2 cells were exposed to 5, 10, 20, 40, and 60  $\mu\text{M}$  of each complex for 24 h, and then, they were analyzed by the MTT assay. Dimethyl sulfoxide (DMSO)-treated cells were classified as control group. The result is shown in Figure 9. For A549 cells, complexes (2) and (3) were found with similar growth-suppressive activity, leading to only 47.09, and 40.26% suppression at 60  $\mu\text{M}$ , respectively. However, complex (1) showed 75.70% suppression at 20  $\mu\text{M}$  after 24 h of treatment. And the  $\text{IC}_{50}$  of complex (1) is 8.82  $\mu\text{M}$ . When Caco-2 cells were used, complexes (1) and (2) were found exhibiting a similar growth-suppressive activity, leading to 72.70 and 59.57%

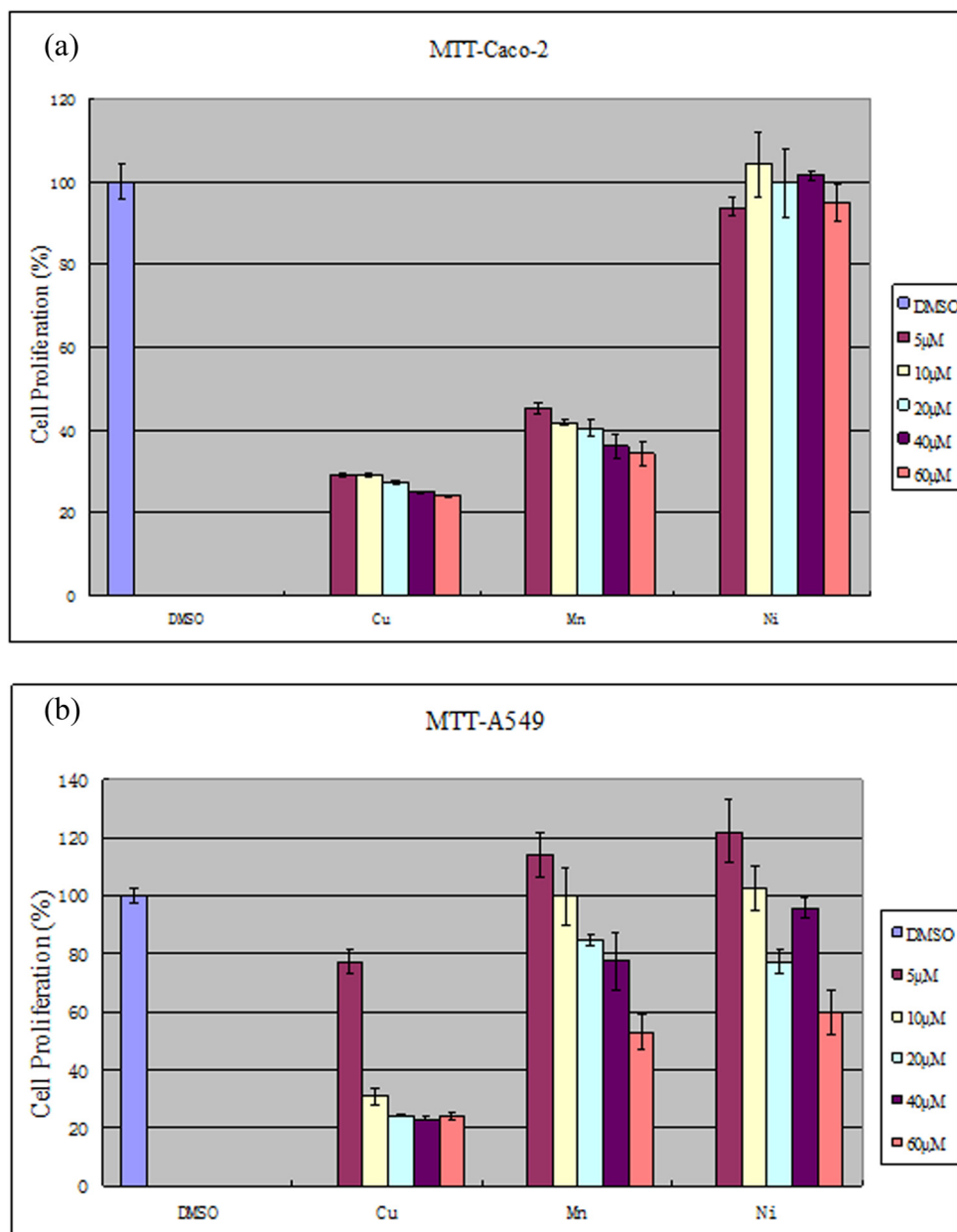


Figure 9: 2,3-(4,5-Dimethylthiazol-2-yl)-2,5-diphenyltetrazolium bromide (MTT) assay for Caco-2 cells (a) and A549 cells (b).

suppression at 20  $\mu\text{M}$ . At 60  $\mu\text{M}$ , however, complex (3) triggered less than 5.02% suppression. And the  $\text{IC}_{50}$  of complexes (1) and (2) is 0.00053 and 1.69  $\mu\text{M}$ , respectively.

It has also been reported that some copper and cadmium complexes can inhibit proteasomes and induce apoptosis in cancer cells. Proteasome inhibition might be effective strategy in anticancer therapy due to the fact that the cancer cells are much more dependent on these processes as compared to normal cells, and proteasome inhibition leads to apoptosis selectively in cancer cells. We will further investigate the mechanism by which complex (1) acts as inhibitors of proteasome activity to induce apoptosis in tumor cells.

## 3 Conclusion

Three complexes, namely  $\text{C}_{52}\text{H}_{28}\text{Cl}_4\text{Cu}_2\text{N}_8\text{O}_{16}\cdot 2\text{CH}_3\text{OH}$  (1),  $\text{C}_{38}\text{H}_{22}\text{Cl}_2\text{MnN}_6\text{O}_8$  (2), and  $\text{C}_{26}\text{H}_{20}\text{Cl}_2\text{NiO}_{10}$  (3), were fabricated and characterized by X-ray diffraction, thermogravimetric study, and elemental study. For complex (1), the crystal crystallizes in triclinic, suggesting that it is a binuclear  $\text{Cu}(\text{II})$  complex. For complex (2), the crystal crystallizes in orthorhombic, revealing that it is a neutral mononuclear complex. For complex (3), the crystal crystallizes in monoclinic, suggesting that it is also a neutral mononuclear complex.

In the presence of  $\text{N}_2$ , the thermal analysis of the complexes was conducted at a temperature from 25 to 1,000°C. Based on their curves, compounds (1), (2), and (3) have thermal stability up to 226, 270, and 120°C, respectively.

The anti-tumor activity of three metal complexes was studied. It was found that complex (1) can induce the proliferation of A549 cells and Caco-2 cells, and complex (2) can induce the proliferation of Caco-2 cells. The results suggest that metal complexes with 2-chloro-5-nitrobenzoic acid and heterocyclic compounds could be developed into new anticancer drugs.

## 4 Experimental

### 4.1 Materials and physical measurement

In the present study, all chemicals were applied without purification. 1,10-Phenanthroline, 2,2'-dipyridyl, and 2-chloro-5-nitrobenzoic acid were bought from Aladdin. DMSO and MTT were bought from Sigma-Aldrich. All metal complexes were prepared as 50 mM stocks in DMSO and deposited at 4°C. FBS was bought from Aleken Biologicals. RPMI-1640,

DMEM/F12 (1:1), and penicillin/streptomycin were bought from Invitrogen.

The elemental analysis was conducted with a 2400 PerkinElmer analyzer [28]. The X-ray diffraction data were collected with a Bruker Smart CCD single-crystal X-ray diffractometer. Thermogravimetric measurements were performed using a METTLER TGA/DSC 3 + instrument. The programmed heating rate was 15°C  $\text{min}^{-1}$ , the protection flow was  $\text{N}_2$ , and the flow rate was 40  $\text{mL min}^{-1}$ . Infrared spectra were recorded as KBr pellets on a Nicolet 170SX spectrophotometer in the 4,000–400  $\text{cm}^{-1}$  region. The UV spectra were performed on a Unicam UV2 spectrometer. Molar conductivity was measured with a WTWLF model 330 conductivity meters, using a prepared solution of the complex in DMSO.

### 4.2 Preparation of complexes

2.0 mmol of 2-chloro-5-nitrobenzoic acid was dissolved in 30.0 mL of anhydrous methanol. 1.0 mmol of metal salt [ $\text{M}(\text{OAc})_2\cdot n\text{H}_2\text{O}$   $\text{M} = \text{Cu}(\text{II})$ ,  $\text{Mn}(\text{II})$ , and  $\text{Ni}(\text{II})$ ] was dissolved in 20.0 mL of anhydrous methanol. The solution of metal salt was dripped in the above 2-chloro-5-nitrobenzoic acid solution and then stirred at 55°C for 4 h. Subsequently, 1.0 mmol of the second ligand (1,10-phenanthroline or 2,2'-dipyridyl) was dissolved in 10.0 mL of anhydrous methanol. The solution of the second ligand was dripped in the above solution and stirred at 55°C for 4 h. Then, the experiment was stopped, cooled to ambient temperature, and filtered. The filtrate evaporates slowly at ambient temperature. Twenty days later, the crystals were formed.

#### 4.2.1 Copper complex (1)

The overall yield of the reaction was 60%. Anal. calc. (%) for  $\text{C}_{52}\text{H}_{28}\text{Cl}_4\text{Cu}_2\text{N}_8\text{O}_{16}\cdot 2\text{CH}_3\text{OH}$  (1): N, 8.278; H, 2.68; C, 47.90. Found (%): N, 8.26; H, 2.70; C, 47.95. UV:  $\lambda_{\text{max}}$  (nm): 241, 306. IR data (KBr,  $\text{cm}^{-1}$ ): 3419.68,  $\nu(\text{OH})$ ; 1500.36,  $\nu_{\text{as}}(-\text{NO}_2)$ ; 1330.01,  $\nu_{\text{s}}(-\text{NO}_2)$ ; 1628.36,  $\nu_{\text{as}}(\text{COO}-)$ ; 1437.68,  $\nu_{\text{s}}(\text{COO}-)$ ; 507.82,  $\nu(\text{Cu-N})$ ; 438.69,  $\nu(\text{Cu-O})$ .

#### 4.2.2 Manganese complex (2)

The overall yield of the reaction was 63%. Anal. calc. (%) for  $\text{C}_{38}\text{H}_{22}\text{Cl}_2\text{MnN}_6\text{O}_8$  (2): N, 10.29; H, 2.71; C, 55.90. Found (%): N, 10.27; H, 2.74; C, 55.93. UV:  $\lambda_{\text{max}}$  (nm): 249, 302. IR data (KBr,  $\text{cm}^{-1}$ ): 1508.42,  $\nu_{\text{as}}(-\text{NO}_2)$ ;

**Table 3:** Crystallographic data and structure refinement for complexes

Identification code	Complex (1)	Complex (2)	Complex (3)
Nomenclature	(1,10-Phenanthroline- $\kappa^2N,N'$ )-di (2-chloro-5-nitrobenzoat)- $\kappa^2O:O$ -bis (2-chloro-5-nitrobenzoic acid- $\kappa^1O$ ) copper (II)-methanol (2/2)	Bis (1,10-phenanthroline- $\kappa^2N,N'$ )-bis (2-chloro-5-nitrobenzoat- $\kappa^1O$ ) manganese(II)	(2,2'-Dipyridyl- $\kappa^2N,N'$ )-bis (2-chloro-5-nitrobenzoat - $\kappa^1O$ )-bis (methanol) nickel(II)
Empirical formula	$C_{54}H_{36}Cl_4Cu_2N_8O_{18}$	$C_{38}H_{22}Cl_2MnN_6O_8$	$C_{26}H_{20}Cl_2N_4NiO_{10}$
Formula weight	1353.79	816.45	678.07
Temperature/K	296.15	296 (2)	296.15
Crystal system	Triclinic	Orthorhombic	Monoclinic
Space group	$P\bar{1}$	$Pna2_1$	$C2/c$
$a/\text{\AA}$	9.905 (7)	17.881 (3)	6.617 (6)
$b/\text{\AA}$	11.685 (10)	10.5472 (17)	29.36 (3)
$c/\text{\AA}$	13.049 (11)	18.318 (3)	14.453 (12)
$\alpha/^\circ$	64.996 (12)	90	90
$\beta/^\circ$	79.725 (15)	90	101.514 (11)
$\gamma/^\circ$	84.949 (13)	90	90
Volume/ $\text{\AA}^3$	1346.6 (19)	3454.7 (10)	2751 (4)
$Z$	1	4	4
$\rho_{\text{calc}}/\text{g cm}^{-3}$	1.669	1.570	1.637
$\mu/\text{mm}^{-1}$	1.074	0.603	0.965
$F(000)$	686.0	1660.0	1384.0
Crystal size/ $\text{mm}^3$	$0.27 \times 0.25 \times 0.23$	$0.24 \times 0.23 \times 0.21$	$0.23 \times 0.2 \times 0.18$
Radiation	MoK $\alpha$ ( $\lambda = 0.71073$ )	MoK $\alpha$ ( $\lambda = 0.71073$ )	MoK $\alpha$ ( $\lambda = 0.71073$ )
$2\theta$ range for data collection/ $^\circ$	3.486–51.012	4.448–49.998	3.996–52.142
Index ranges	$-9 \leq h \leq 11, -14 \leq k \leq 13, -15 \leq l \leq 15$	$-20 \leq h \leq 21, -10 \leq k \leq 12, -21 \leq l \leq 19$	$-7 \leq h \leq 8, -25 \leq k \leq 36, -17 \leq l \leq 17$
Reflections collected	7,848	19,531	8,306
Independent reflections	4980 [ $R_{\text{int}} = 0.0542, R_{\text{sigma}} = 0.1033$ ]	5791 [ $R_{\text{int}} = 0.0326, R_{\text{sigma}} = 0.0367$ ]	2690 [ $R_{\text{int}} = 0.0971, R_{\text{sigma}} = 0.1080$ ]
Data/restraints/parameters	4,980/7/390	5,791/1/496	2,690/0/196
Goodness-of-fit on $F^2$	0.952	1.025	1.122
Final $R$ indexes [ $I > 2\sigma(I)$ ]	$R_1 = 0.0599, wR_2 = 0.1387$	$R_1 = 0.0293, wR_2 = 0.0611$	$R_1 = 0.1058, wR_2 = 0.2897$
Final $R$ indexes [all data]	$R_1 = 0.1083, wR_2 = 0.1687$	$R_1 = 0.0403, wR_2 = 0.0665$	$R_1 = 0.1375, wR_2 = 0.3055$
Largest diff. peak/hole/ $e \text{\AA}^{-3}$	0.73/–0.70	0.20/–0.22	1.31/–0.79

1321.17,  $\nu_s(-\text{NO}_2)$ ; 1630.78,  $\nu_{\text{as}}(\text{COO}-)$ ; 1432.26,  $\nu_s(\text{COO}-)$ ; 510.32,  $\nu(\text{Mn}-\text{N})$ ; 440.13,  $\nu(\text{Mn}-\text{O})$ .

#### 4.2.3 Nickel complex (3)

The overall yield of the reaction was 70%. Anal. calc. (%) for  $C_{26}H_{20}Cl_2N_4NiO_{10}$  (3): N, 8.26; H, 2.97; C, 46.05. Found (%): N, 8.30; H, 2.99; C, 46.02. UV:  $\lambda_{\text{max}}$  (nm): 250, 301. IR data (KBr,  $\text{cm}^{-1}$ ): 1510.37,  $\nu_{\text{as}}(-\text{NO}_2)$ ; 1341.17,  $\nu_s(-\text{NO}_2)$ ; 1631.69,  $\nu_{\text{as}}(\text{COO}-)$ ; 1440.58,  $\nu_s(\text{COO}-)$ ; 498.21,  $\nu(\text{Ni}-\text{N})$ ; 429.73,  $\nu(\text{Ni}-\text{O})$ .

### 4.3 Crystallographic data collection and structure determination

Under a graphite monochromatic Mo-K $\alpha$  radiation at 298(2) K, we collected X-ray diffraction data with a Bruker Smart CCD diffractometer. Data were collected in a series of  $\omega$ - $2\theta$  scan. The crystal structure was solved directly by SHELXS-97 [29]. Non-hydrogen atoms were defined by Fourier synthesis. To refine the position parameters and thermal parameters to make them converge, the full matrix least square method was employed. Crystallographic information is listed in Table 3 [30].

## 4.4 Cell culture

Caco-2 human colon adenocarcinoma cells and A549 human lung cancer cells originated from the American Type Culture Collection. A549 cells and Caco-2 cells underwent incubation in RPMI-1640 medium and DMEM/F-12 (1:1) medium, respectively. All media were added with 100 µg/mL of streptomycin, 10% FBS, and 100 U/mL of penicillin. All cells were incubated in a humidified environment with 5% CO<sub>2</sub> at 37°C [31].

## 4.5 Cell proliferation assay

MTT assay was performed for the detection of the effects of metal complexes on cell proliferation. In brief, A549 cancer cells and Caco-2 cancer cells were seeded in a 96-well plate in triplicate and then incubated to 70–80% confluent at 37°C. Subsequently, the indicated concentrations of the complexes were exploited to treat cancer cells for 24 h [32]. The culture medium was removed, and MTT solution (1 mg/mL) was introduced for 2 h. Subsequently, MTT solution was removed, and 100 µL of DMSO was introduced to dissolve the metabolite formazan. Finally, the absorbance value was measured with the Victor 3 multi-label plate reader.

**Funding information:** This research was supported by the Bidding subject of Dezhou University (No. 3010040205), the Talent Introduction Program of Dezhou University (No. 2016kjrc17), and the National Natural Science Foundation of China (No. 21806019).

**Conflict of interest:** Authors state no conflict of interest.

**Data availability statement:** The datasets generated during and/or analyzed during the current study are available from the corresponding author on reasonable request.

## References

- [1] Lee CK, Park KK, Lim SS, Park JHY, Chung WY. Effects of the licorice extract against tumor growth and cisplatin-induced toxicity in a mouse xenograft model of colon cancer. *Biol Pharm Bull.* 2015;309(11):2191–5.
- [2] Rose PG, Bundy BN, Watkins EB, Thigpen JT, Deppe G, Maiman MA, et al. Concurrent cisplatin-based radiotherapy and chemotherapy for locally advanced cervical cancer. *N Engl J Med.* 1999;340(15):1144–53.
- [3] Giaccone G. Gefitinib in combination with gemcitabine and cisplatin in advanced non-small-cell lung cancer: a phase III trial – INTACT 1. *J Clin Oncol.* 2004;22(5):777–84.
- [4] Tiseo M, Martelli O, Mancuso A, Sormani MP, Bruzzi P, Di SR, et al. Short hydration regimen and nephrotoxicity of intermediate to high-dose cisplatin-based chemotherapy for out-patient treatment in lung cancer and mesothelioma. *Tumori.* 2007;93(2):138–44.
- [5] Nematbakhsh M, Nasri H, Talebi A, Pilehvarian AA, Safari T, Eshraghi-Jazi F, et al. Evidence against protective role of sex hormone estrogen in cisplatin-induced nephrotoxicity in ovariectomized rat model. *Toxicol Int.* 2013;20(1):43–7.
- [6] Gailer J. Improving the safety of metal-based drugs by tuning their metabolism with chemoprotective agents. *Bioinorg Chem.* 2017;179:154–7.
- [7] Newkome GR, Marston CR. Chemistry of heterocyclic compounds series. 110. Cobalt-60. gamma-irradiation:homolytic alkylation of methyl nicotinate. *J Inorg Chem.* 1985;50(21):4162–3.
- [8] Lage H, Aki-Sener E, Yalcin I. High antineoplastic activity of new heterocyclic compounds in cancer cells with resistance against classical DNA topoisomerase II-targeting drugs. *Int J Cancer.* 2010;119(1):213–20.
- [9] Zhang Z, Bi C, Fan Y, Zhang X, Zhang N, Yan X, et al. Crystal structure, fluorescence property and theoretical calculation of the Zn(II) complex with o-aminobenzoic acid and 1,10-phenanthroline. *Bull Korean Chem Soc.* 2014;35(6):1697–702.
- [10] Ji NN, Shi ZQ, Zhao RG, Zheng ZB, Li ZF. Synthesis, crystal structure and quantum chemistry of a novel Schiff base N-(2,4-dinitro-phenyl)-N'-(1-phenyl-ethylidene)-hydrazine. *Bull Korean Chem Soc.* 2010;31(4):881–6.
- [11] Shibata J, Murakami K, Wierzbka K, Aoyagi Y, Hashimoto A, Sano M, et al. Anticancer effect of 4-[3,5-bis(trimethylsilyl)benzamido] benzoic acid (TAC-101) against A549 non-small cell lung cancer cell line is related to its anti-invasive activity. *Anticancer Res.* 2000;20(5A):3169–76.
- [12] Xie WL, Yang PH, Zeng X, Cai JY. Effect of 4-(12-dihydroartemisininoxy) benzoic acid hydrazide transferrin tagged drug on human breast cancer cells. *Chinese J Anal Chem.* 2009;37(5):671–5.
- [13] Singh A, Sharma RP, Aree T, Venugopalan P. Weak C–H...F–C interactions in carboxylate anion binding: synthesis, spectroscopic and X-ray structural studies of [Co(phen)<sub>2</sub>CO<sub>3</sub>] (C<sub>7</sub>H<sub>3</sub>O<sub>2</sub>Cl)Cl·11H<sub>2</sub>O and [Co(phen)<sub>2</sub>CO<sub>3</sub>](C<sub>7</sub>H<sub>3</sub>NO<sub>4</sub>Cl)·6H<sub>2</sub>O. *J Chem Sci.* 2010;122(5):739–50.
- [14] Ferenc W, Walkow-Dziewulska A, Cristovao B, Sarzynski J. Magnetic, spectrochemical and thermal properties of the 2-chloro-5-nitrobenzoates of Co(II), Ni(II) and Cu(II). *J Serb Chem Soc.* 2006;71(8/9):929–37.
- [15] Milani NC, Maghsoud Y, Hosseini M, Babaei A, Gholivand K. A new class of copper (I) complexes with imine-containing chelators which show potent anticancer activity. *Appl Organometal Chem.* 2020;34(4):e5526.
- [16] Tanaka K, Furo M, Ihara E, Yasuda H. Unique dual function of La (C<sub>5</sub>Me<sub>5</sub>)[CH(SiMe<sub>3</sub>)<sub>2</sub>]<sub>2</sub>(THF) for polymerizations of both non-polar and polar monomers. *J Polym Sci Part A: Polym Chem.* 2001;39(9):1382–90.
- [17] Sharma RP, Saini A, Monga D, Venugopalan P, Jezierska J, Ozarowski A, et al. Influence of nitrogen donor ligands on the coordination modes of copper(II) 2-nitrobenzoate complexes:

- structures, DFT calculations and magnetic properties. *New J Chem.* 2013;38(1):437–47.
- [18] Tidwell CP, Bharara P, Rudeseal TA, Rudeseal GM, Belmore K, Bailey MJ, et al. Synthesis and characterization of 5,10,15,20-Tetrakis[3-(3,4-dichlorophenoxy)]porphyrin and some of its metal complexes. *Heterocycl Commun.* 2007;13(6):353–8.
- [19] de Hoog P, Gamez P, Mutikainen I, Reedijk Turpeinen U. An aromatic anion receptor: anion- $\pi$  interactions do exist. *Angew Chem.* 2004;116:5939–41.
- [20] Wolińska E, Karczmarzyk Z, Wysocki W. Structural characterization of copper complexes with chiral 1,2,4-triazine-oxazoline ligands. *Heterocycl Commun.* 2016;22(5):265–74.
- [21] Pschirer NG, Ciurtin DM, Smith MD, Bunz UHF, Loye HZ. Noninterpenetrating square-grid coordination polymers with dimensions of  $25 \times 25 \text{ Å}^2$  prepared by using N,N'-type ligands: the first chiral square-grid coordination polymer. *Angew Chem.* 2002;114(4):603–5.
- [22] Huang GM, Zhang X, Fan YH, Bi CF, Yan XC, Zhang ZY, et al. Synthesis, crystal structure and theoretical calculation of a novel nickel(II) complex with dibromotyrosine and 1,10-phenanthroline. *Bull Korean Chem Soc.* 2013;34(10):2889–94.
- [23] Jassal AK, Sharma S, Hundal G, Hundal MS. Structural diversity, thermal studies, and luminescent properties of metal complexes of dinitrobenzoates: a single crystal to single crystal transformation from dimeric to polymeric complex of copper(II). *Cryst Growth Des.* 2015;15(1):79–93.
- [24] Nemcova B, Mikulaskova H, Bednarova I, Beklova M, Pikula J. Impact of platinum group elements on the soil invertebrate *Folsomia candida*. *Neuroendocrinol Lett.* 2013;34(2):5–10.
- [25] Chen D, Daniel KG, Chen MS, Kuhn DJ, Landis-Piwowar KR, Dou QP. Dietary flavonoids as proteasome inhibitors and apoptosis inducers in human leukemia cells. *Biochem Pharmacol.* 2005;69(10):1421–32.
- [26] Zhang Z, Bi C, Fan Y, Zhang N, Deshmukh R, Yan X, et al. L-Ornithine Schiff base-copper and -cadmium complexes as new proteasome inhibitors and apoptosis inducers in human cancer cells. *J Biol Inorg Chem.* 2013;20:109–21.
- [27] Daniel KG, Chen D, Orlu S, Cui Q, Miller FR, Dou QP. Clotquinol and pyrrolidine dithiocarbamate complex with copper to form proteasome inhibitors and apoptosis inducers in human breast cancer cells. *Breast Cancer Res.* 2005;7(6):897–908.
- [28] Micale N, Sarro GD, Ferreri G, Zappalá M, Grasso S, Puia G, et al. Design of 1-substituted 2-arylmethyl-4,5-methylene-dioxybenzene derivatives as antiseizure agents. *Bioorg Med Chem.* 2004;12(13):3703–9.
- [29] Sheldrick GM. SHELXTL-97, program for crystal structure refinement. Germany: University of Göttingen; 1997.
- [30] Morrison RM, Thompson RC, Trotter J. The molecular and crystal structure of tetrakis(4-methylpyridine)cobal(II) hexafluorophosphate. *Can J Chem.* 2011;57(2):135–8.
- [31] Motaghd M, AlHassan FM, Hamid SS. Thymoquinone regulates gene expression levels in the estrogen metabolic and interferon pathways in MCF7 breast cancer cells. *Int J Mol Med.* 2014;33(1):8–16.
- [32] Tsuji S, Tsuura Y, Morohoshi T, Shinohara T, Oshita F, Yamada K, et al. Secretion of intelectin-1 from malignant pleural mesothelioma into pleural effusion. *Br J Cancer.* 2010;103(4):517–23.